The Residue Composition of the Aromatic Anchor of the Second Transmembrane Helix Determines the Signaling Properties of the Aspartate/Maltose Chemoreceptor Tar of Escherichia coli

ARTICLE *in* BIOCHEMISTRY · MARCH 2012

Impact Factor: 3.02 · DOI: 10.1021/bi201555x · Source: PubMed

3 AUTHORS, INCLUDING:

Roger Draheim
University of Portsmouth
16 PUBLICATIONS **433** CITATIONS

SEE PROFILE

BIOCHEMISTRY
including biophysical chemistry & molecular biology

Article

pubs.acs.org/biochemistry

The Residue Composition of the Aromatic Anchor of the Second Transmembrane Helix Determines the Signaling Properties of the Aspartate/Maltose Chemoreceptor Tar of *Escherichia coli*

Christopher A. Adase,[†] Roger R. Draheim,[‡,§] and Michael D. Manson*[,†]

[†]Department of Biology, Texas A&M University, College Station, Texas 77843, United States

[‡]Department of Biochemistry and Biophysics, The Arrhenius Laboratories for Natural Sciences, Stockholm University, Stockholm SE-10691, Sweden

[§]Institute of Biochemistry, Biocenter, Goethe University Frankfurt, D-60438 Frankfurt, Germany

Supporting Information

ABSTRACT: Repositioning of the tandem aromatic residues (Trp-209 and Tyr-210) at the cytoplasmic end of the second transmembrane helix (TM2) modulates the signal output of the aspartate/maltose chemoreceptor of *Escherichia coli* (Tar_{Ec}). Here, we directly assessed the effect of the residue composition of the aromatic anchor by studying the function of a library of Tar_{Ec} variants that possess all possible combinations of Ala, Phe, Tyr, and Trp at positions 209 and 210. We identified three important properties of the aromatic anchor. First, a Trp residue at position 209 was required to maintain clockwise (CW) signal output in the absence of adaptive methylation, but adaptive methylation restored the ability of all of the mutant receptors to generate CW rotation. Second, when the aromatic anchor was replaced with tandem Ala residues, signaling was less compromised than when an Ala residue occupied position 209 and an aromatic residue occupied position 210. Finally, when Trp was present at position 209, the identity of the residue at position 210 had little effect on baseline signal output or aspartate chemotaxis, although maltose taxis was significantly affected by some substitutions at position 210. All of the mutant receptors we constructed supported some level of aspartate and maltose taxis in semisolid agar swim plates, but those without Trp at position 209 were overmethylated in their baseline signaling state. These results show the importance of the cytoplasmic aromatic anchor of TM2 in maintaining the baseline Tar_{Ec} signal output and responsiveness to attractant signaling.

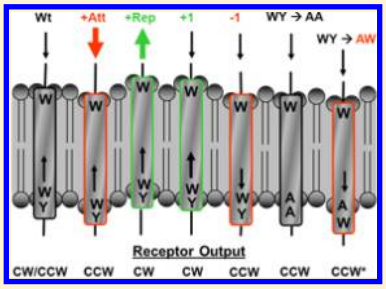

In a chemically homogeneous environment, *Escherichia coli* moves in a three-dimensional random walk that consists of a series of smooth-swimming "runs" interspersed with brief "tumbles" that reorient the bacterium in three-dimensional space. Runs are produced when the flagella rotate counterclockwise (CCW), which causes the left-handed helical flagellar filaments to coalesce into a bundle at one end of the cell.[1,2] Tumbles occur when one or more flagella switch from CCW to clockwise (CW) rotation, which disrupts the helical bundle and causes a random reorientation of the cell.[2]

E. coli possesses several transmembrane chemoreceptors, known as methyl-accepting chemotaxis proteins (MCPs), that mediate behavioral responses to specific sets of compounds. These MCPs, along with the aerotaxis (Aer) receptor, utilize a common signal transduction pathway that modulates the rotational bias of the motors of the flagella. By decreasing CCW rotation, a cell can extend the duration of runs in a favorable direction, either up an attractant gradient or down a repellent gradient.[3,4]

Attractant binding induces covalent modification of the cognate MCP.[5] Methyl groups are added by a methyltransferase, CheR, and removed by a methylesterase, CheB.[6,7] CheB also removes the amide groups from the two glutaminyl residues that comprise two of the modification sites in the newly translated protein.[8] An increased level of methylation of eight specific glutamyl residues (four per subunit) within the receptor homodimer stimulates the activity of the CheA kinase, whereas a decreased level of methylation weakens CheA stimulation.[9]

The aspartate chemoreceptor of *E. coli* (Tar_{Ec}) detects the presence of attractants both directly (aspartate) and indirectly (maltose). Aspartate binds at one of two rotationally symmetric binding sites in the periplasmic domain of the Tar_{Ec} homodimer. Maltose first associates with the periplasmic maltose-binding protein (MBP), causing MBP to adopt a conformation that facilitates interaction with Tar_{Ec}.[10,11] Maltose-bound MBP binds to the apex of the Tar periplasmic four-helix bundle.[12,13] Tar_{Ec} also mediates repellent taxis to Ni^{2+} and Co^{2+}, which also bind directly to its periplasmic domain.[14,15]

E. coli MCPs contain two transmembrane helices. Transmembrane helix 1 (TM1) is an N-terminal extension of helix 1 of the periplasmic domain. Transmembrane helix 2 (TM2) is a C-terminal extension of helix 4 of that domain. TM2

Received: October 9, 2011
Revised: January 11, 2012
Published: February 17, 2012

   dx.doi.org/10.1021/bi201555x | *Biochemistry* 2012, 51, 1925−1932

communicates the conformational change induced by ligand binding to the cytoplasmic HAMP domain (histidine kinases, adenylyl cyclases, methyl-accepting chemotaxis proteins, and certain phosphatases).[16] The mechanism of signal transduction from the periplasmic domain to the HAMP domain is not fully understood, but several hypotheses have been advanced to explain the process.[17−19] Whatever the signaling mechanism may be, the preponderance of evidence suggests that a small (∼1−3 Å) inward displacement of helix 4 of TM2 roughly perpendicular to the plane of the membrane occurs upon binding of aspartate.[20−26]

Repositioning the two aromatic residues (the aromatic anchor) at the cytoplasmic end of TM2 of Tar_{Ec} (Trp-209 and Tyr-210) by a single position is sufficient to modulate the signal output of Tar_{Ec}.[26] Mutant receptors in which the aromatic anchor was moved toward the hydrophobic core of the membrane had decreased CW signal output. This suggests that the well-documented affinity of amphipathic aromatic residues for the polar−hydrophobic interfaces[27−29] within the phospholipid bilayer is sufficient to reposition TM2 toward the cytoplasm in a manner similar to an aspartate-induced displacement.[20−26] Conversely, mutant receptors in which the aromatic anchor was repositioned toward the polar headgroups exhibit increased CW signal output,[26] a result consistent with displacement of TM2 from the cytoplasm. These results demonstrate that aromatic residues can "tune" the output of Tar_{Ec}, and perhaps those of other chemoreceptors and members of the sensor histidine kinase superfamily that share a similar mechanism of transmembrane communication.[30−33]

A variety of chemoreceptors and other two-pass transmembrane sensor proteins have aromatic residues at the cytoplasmic end of TM2 followed by a HAMP domain (Table S1 of the Supporting Information). To determine the essential features of the cytoplasmic aromatic anchor of Tar_{Ec}, Trp-209 and Tyr-210 were replaced with all possible combinations of other aromatic residues and Ala. We also looked at the effect of introducing a variety of different residues at position 210 when Trp-209 was still present. Our results indicate that Trp-209 is crucial for the ability of Tar_{Ec} to stimulate CheA activity in a Δ*cheRB* strain. However, adaptive covalent modification can restore sufficient function to allow chemotaxis. When Trp-209 is present, charged or polar uncharged amino acids at position 210 impair function to some extent, but the effect is smaller than that accompanying the loss of Trp-209. Thus, the optimal function of Tar_{Ec} requires a cytoplasmic aromatic anchor with a WX configuration, where X is a nonpolar residue.

MATERIALS AND METHODS

Bacterial Strains and Plasmids. HCB436 [Δ*tsr7021* Δ*trg100* Δ(*tar-cheB*)*2234*],[34] RP3098 [Δ(*flhD-flhB*)*4*],[35] and VB13 (Δ*tsr7021* Δ*tar-tap5201 trg*::Tn*10*)[36] are derived from *E. coli* K-12 strain RP437.[37] Strain VB13 is deleted for all chemoreceptor genes, as is strain HCB436, which also carries a Δ*cheRcheB* deletion. All in vivo assays of receptor activity were conducted with these two strains. Strain RP3098 contains a deletion of the master regulator *flhDC* and therefore fails to produce any Che proteins. Plasmid pRD200,[25] derived from pMK113,[13] was used to express wild-type or mutant *tar* genes constitutively. In addition, an in-frame coding sequence for a seven-residue linker (GGSSAAG)[38] and a C-terminal V5 epitope tag (GKPIPNPLLGLDST)[39] was added to the 3′ end of *tar*. Plasmid pRD300[25] is a derivative of pBAD18[40] that expresses *tar* with the same C-terminal linker and V5 epitope tag upon induction with L-arabinose. Strain RP3098 was used with pRD300 as previously described[25] to produce standards for the in vivo methylation assay. Mutations in *tar* were introduced via site-directed mutagenesis (Stratagene).

Observation of Tethered Cells. HCB436 or VB13 cells containing plasmid pRD200 were grown overnight in tryptone broth[41] supplemented with 100 μg/mL ampicillin. Overnight cultures were then back-diluted 1:100 in tryptone broth and grown at 30 °C with agitation until OD_{600} reached ∼0.6. A 10 mL aliquot of cells was pelleted, and the cells were resuspended in 10 mL of tethering buffer [10 mM potassium phosphate (pH 7.0), 100 mM NaCl, 10 μM EDTA, 20 μM L-methionine, 20 mM sodium DL-lactate, and 200 μg/mL chloramphenicol]. Flagella were sheared in a Waring blender[42] during eight repetitions of 7 s intervals of shearing at high speed interspersed with 13 s pauses to prevent overheating. Cells were collected by centrifugation, washed three times in tethering buffer, and mixed with an equal volume of a 200-fold dilution of anti-flagellar filament antibody. A 40 μL aliquot of the cell/antibody mix was added to the center of the coverslip. Coverslips were then incubated in a humidity chamber for 30 min at 30 °C and affixed to a flow chamber;[43] nontethered cells were removed by flushing the chamber with chemotaxis buffer. Cells were observed under reverse phase contrast at 1000× magnification, using an Olympus BH-2 microscope. Rotating cells were digitally recorded, and at least 100 cells for each specific receptor were monitored visually during a 20 s playback. Cells were assigned to one of five rotational categories: exclusively CCW, mostly CCW with occasional reversals, reversing frequently with no clear bias, mostly CW with occasional reversals, and exclusively CW. The reversal frequency was determined by tallying the number of reversals for each cell during video playback.

Determination of the Methylation State of Receptors in Vivo. HCB436 or VB13 cells containing plasmid pRD200 expressing each of the different V5-tagged Tar variants were grown overnight at 30 °C in tryptone broth supplemented with 100 μg/mL ampicillin. Overnight cultures were then back-diluted 1:100 in tryptone broth and grown at 30 °C to an OD_{600} of ∼0.6. Cells were harvested by centrifugation, washed three times with 10 mL of 10 mM potassium phosphate buffer (pH 7.0) containing 0.1 mM EDTA, and resuspended in 5 mL of 10 mM potassium phosphate (pH 7.0) containing 0.1 mM EDTA, 10 mM sodium DL-lactate, and 200 μg/mL chloramphenicol. Aliquots (1 mL) were transferred to 10 mL scintillation vials and incubated for 10 min at 32 °C, with agitation. Cells were then incubated for an additional 30 min after the addition of L-methionine to a final concentration of 100 μM. A 100 μL aliquot of 100 mM L-aspartate or 10 mM $NiSO_4$ solutions, or 100 μL of buffer as control, was added at this time, and the cells were incubated for an additional 20 min. Reactions were terminated by addition of 100 μL of ice-cold 100% TCA, and the samples were then incubated on ice for 15 min. Denatured proteins were pelleted, washed with 1% TCA and acetone, and resuspended in 100 μL of 2× SDS loading buffer. A 15 μL aliquot of each sample was subjected to sodium dodecyl sulfate−polyacrylamide gel electrophoresis (SDS−PAGE) and immunoblotting with antibodies raised against the V5 epitope that were conjugated to alkaline phosphatase (Invitrogen). Standards were run as a mixture of Tar proteins containing equal proportions of V5-tagged versions of the EEEE, QEQE, and QQQQ forms of the Tar receptor produced from RP3098 cells containing pRD300. The Gln residues affect

protein migration like methylated Glu residues, so that the standards migrate like the unmethylated, doubly methylated, and quadrupally methylated forms of the receptor, respectively.

Swim-Plate Chemotaxis Assays. Semisolid motility agar contained 3.25 g/L Difco BactoAgar (Difco) in motility medium [10 mM potassium phosphate (pH 7.0), 1 mM $(NH_4)_2SO_4$, 1 mM $MgSO_4$, 1 mM $MgCl_2$, 1 mM glycerol, and 90 mM NaCl] and was supplemented with 20 μg/mL L-threonine, L-histidine, L-methionine, and L-leucine and 1 μg/mL thiamine. Aspartate and maltose were added to final concentrations of 100 μM. Plates were inoculated with toothpicks from isolated colonies of strain VB13 expressing one of the various Tar receptors from pRD200. Swarm plates were incubated at 30 °C. Once chemotaxis rings became visible (typically 8 h for aspartate and 12 h for maltose plates), their diameter was measured every 4 h.

Analysis of Receptor Function in Vitro. Receptor-containing inner membranes were isolated as previously described.[44] Strain RP3098[35] harboring either pRD100[25] expressing the wild-type Tar, or pRD300[25] expressing its C-terminal V5 epitope-tagged variant, was used for production of receptor-containing membranes. Tar expression was induced by the addition of L-arabinose to a final concentration of 0.2% (w/v). Soluble Che proteins were isolated,[44] and receptor-coupled in vitro phosphorylation assays were performed as previously described.[25] Our reaction mixtures contained 20 pmol of Tar, 5 pmol of CheA, 20 pmol of CheW, and 500 pmol of CheY in 9 μL of fresh phosphorylation buffer [50 mM Tris-HCl, 50 mM KCl, 5 mM $MgCl_2$, and 2 mM DTT (pH 7.5)]. Aspartate was added to the desired final concentration, taking care to maintain the same total volume. The reaction was initiated by the addition of 1 μL of [γ-^{32}P]ATP (3000 Ci/mmol, NEN catalog no. BLU502A) diluted 1:1 with 10 mM unlabeled ATP. Reactions were terminated by addition of 40 μL of 2× SDS−PAGE loading buffer containing 25 mM EDTA. Samples were subjected to SDS−PAGE, dried, and imaged using a phosphorimager (Fuji BAS 5000).

RESULTS

The Residue Composition of the Aromatic Anchor Affects the Baseline Tar_{Ec} Signal Output. Fifteen mutant receptors were generated by making all possible substitutions of Ala, Phe, Trp, and Tyr at residues 209 and 210 of Tar_{Ec}, which are Trp and Tyr, respectively, in the wild-type protein. Flagellar rotational bias and mean reversal frequency (MRF) were measured in transducer-depleted (ΔT) tethered cells (strain VB13; Δ*tsr* Δ*tar-tap* Δ*trg aer*$^+$) expressing the wild-type or mutant Tar_{Ec} proteins from plasmid pRD200. The effects of a C-terminal V5 tag on ligand sensitivity and adaptation responses are minimal and have been well characterized (Figure S1 of the Supporting Information).[45] The behavior of these cells should reflect the steady-state Tar_{Ec} signal output, which is modulated by changes both in the position of TM2 relative to the membrane and in the resultant compensatory effects of adaptive methylation.[25,26,46]

VB13 cells expressing V5-tagged wild-type Tar_{Ec} (WY anchor) from pRD200 showed a modest CCW rotational bias (Figure 1). All mutant receptors supported some CW rotation and ranged from slightly more CW-biased (the WA receptor) to somewhat more CCW-biased (all receptors with Ala at position 209 and the FA, FW, YF, and YW receptors). The FF, FY, WF, WW, YA, and YY receptors supported essentially wild-type rotational biases in VB13 cells. The MRF

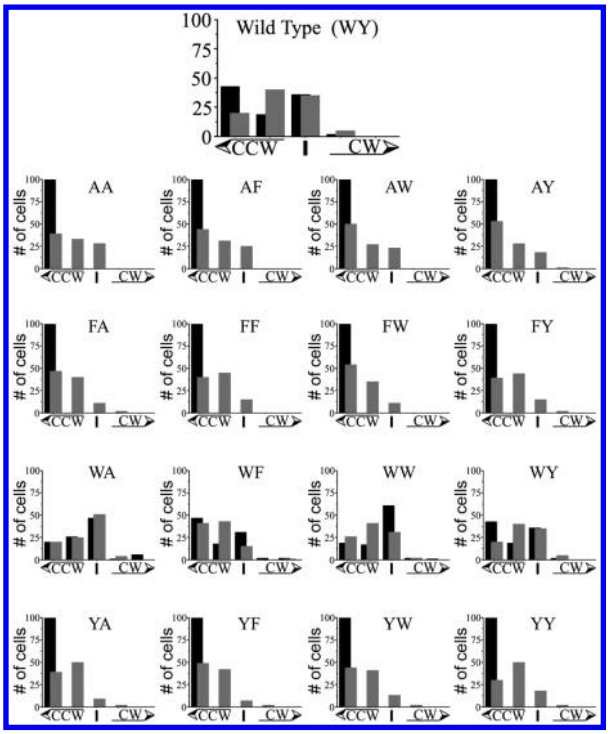

Figure 1. Flagellar rotational bias of cells expressing Tar_{Ec} variants with wild-type or mutant aromatic tandems. VB13 (ΔT *cheR*$^+$*B*$^+$) or HCB436 (ΔT Δ*cheRB*) cells expressing the wild-type or mutant Tar_{Ec} variants from pRD200[25] possessing a C-terminal epitope V5 tag were tethered, observed for 20 s, and assigned to one of five categories based on their apparent flagellar rotational bias. From left to right, these categories are designated counterclockwise rotation with no switching (CCW only), counterclockwise-biased with switching (CCW), frequent reversing with no apparent bias (CCW/CW), clockwise-biased with switching (CW), and clockwise rotation with no switching (CW only). Results from VB13 cells are depicted as gray bars in the foreground, whereas results from HCB436 cells are depicted as black bars in the background. Each histogram contains the classification of 100 VB13 and 100 HCB436 cells expressing a different Tar_{Ec} variant.

values of VB13 cells expressing the mutant receptors (Figure S2 of the Supporting Information) were all between 0.15 and 0.45 s^{-1}, with the highest MRF shown by the WA receptor.

Cells Lacking Adaptive Methylation Cannot Compensate for the Absence of Trp-209. A very different picture emerged when receptor performance was analyzed in strain HCB436,[36] a ΔT strain that also lacks the adaptation enzymes CheR (methyltransferase) and CheB (methylesterase/deamidase). In these cells, the receptors remain in the QEQE modification state in which they are translated. HCB436 cells expressing receptors with Trp at position 209 supported CCW-biased flagellar rotation (Figure 1). The wild-type (WY) and WA receptors had MRF values similar to those in VB13 cells, but the WF and WW receptors expressed in HCB436 cells supported MRF values ∼2 times greater than those seen in VB13 cells (Figure S2 of the Supporting Information). HCB436 cells producing receptors with other residues at positions 209 and 210 never rotated CW. Thus, an intact adaptation system is required to compensate for the inherently CCW-locked baseline signal output of these mutant receptors.

Adaptive Methylation Compensates for Changes in the Residue Composition of the Anchor. The level of in vivo covalent modification for all of the receptor variants was

dx.doi.org/10.1021/bi201555x | *Biochemistry* 2012, 51, 1925−1932

examined. In strain HCB436, all 16 proteins migrated as a single band with the same motility as wild-type Tar (Figure S3 of the Supporting Information). In VB13 cells, all of the receptors with Trp at position 209 migrated as two bands, probably representing the EEEE and singly methylated forms. The WA receptor was shifted slightly toward the least-modified band. In contrast, all but one of the other mutant receptors showed significantly higher levels of covalent modification in their baseline states (Figure S3 of the Supporting Information). All of the receptors responded to the addition of 10 mM aspartate by increasing their levels of covalent modification, and all except the WA receptor responded to 10 mM $NiSO_4$ by decreasing their levels of covalent modification (Figure S4 of the Supporting Information).

We classified the proteins into three categories with respect to their baseline and attractant-adapted levels of covalent modification (Figure 2): wild-type, overmethylated, and highly

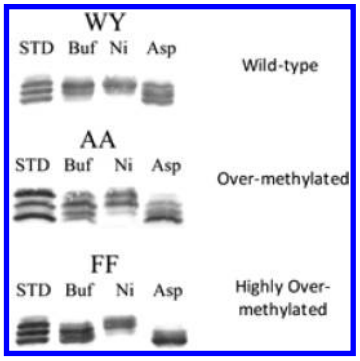

Figure 2. Examples of band migration patterns for Tar_{Ec} variants from each category of covalent modification state. Tar_{Ec} variants were clustered into three groups depending on the degree of modification in the baseline signaling state and in the presence of the repellent Ni^{2+} and the attractant aspartate. The wild-type anchor (WY) is shown for the wild-type class. Tar_{Ec} with the AA anchor represents a moderate increase (overmethylated) in baseline and aspartate-induced modification states. Tar_{Ec} with the FF anchor represents a greater increase (highly overmethylated) in the baseline and aspartate-induced modification states.

overmethylated. Despite the binning into discrete groups imposed by this classification, the receptors actually were distributed along a continuum of modification states.

Four variants showed levels of covalent modification comparable to those of the wild-type WY receptor. We included the WF, WW, WA, and YA receptors in this class, although the WA receptor was somewhat less modified and the YA receptor was slightly more modified than the wild-type receptor (Figure S3 of the Supporting Information). Receptors of the second class, exemplified by the AA receptor in Figure 2, were significantly more modified in the baseline state and showed more extensive modification in the presence of aspartate. This class included the AA, AF, AY, FA, FW, and FY receptors. Finally, the highly overmethylated class consisted of the AW, FF, YF, YW, and YY receptors. They were highly modified in the baseline state, and their level of modification increased even more after the addition of aspartate. This third class of receptors decreased the level of modification after the addition of $NiSO_4$. The overall conclusion is that the increases in CCW signaling bias of all receptors are within a range that can be largely accommodated by the adaptation system.

The Extent of Adaptive Methylation Required To Maintain the Baseline Tar_{Ec} Signal Output Correlates with the Rate of Chemotaxis Ring Expansion in Semisolid (swim) Agar. All 16 receptors were examined for their ability to support chemotaxis to aspartate and maltose in VB13 cells. The expansion rates of chemotaxis rings in semisolid agar containing 100 μM aspartate or 100 μM maltose were calculated (Figure 3 and Table 1). All receptors with Trp

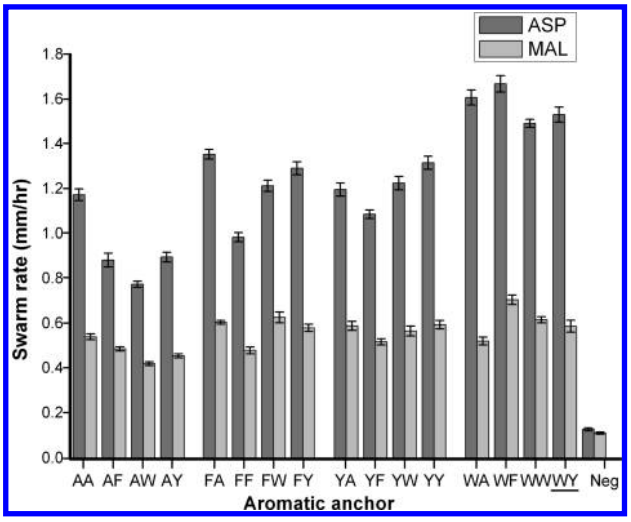

Figure 3. Chemotaxis ring formation in aspartate and maltose swim plates by cells expressing Tar_{Ec} variants containing different aromatic anchors. VB13 (ΔT $cheR^+B^+$) cells expressing wild-type Tar_{Ec} or different Tar_{Ec} variants from pRD200[25] were inoculated into semisolid agar containing aspartate or maltose. Plates were incubated at 30 °C and measured after 8 h, when migratory rings first became visible. The ring diameter was measured every 4 h thereafter, and the migration rate was calculated in millimeters per hour. The error bars show the standard error of the mean for the expansion rates of ≥18 colonies. The wild-type anchor (WY) is underlined.

at position 209 were as good as wild-type Tar_{Ec} at supporting aspartate taxis, with expansion rates ranging from 1.49 mm/h for the wild type to 1.67 mm/h for the WF variant. None of the other variants supported ring expansion rates above 1.32 mm/h. The three slowest rates, ~0.8 mm/h, were exhibited by the AY, AF, and AW receptors. Even though the rate of migration between mutants varies significantly, all mutants produce migratory rings with a similar appearance (Figure S5 of the Supporting Information).

The rates of ring expansion in maltose semisolid agar generally correlated with those for aspartate, with the fastest rate of 0.7 mm/h supported by the WF variant and the slowest rates of 0.42–0.49 mm/h exhibited by the AY, AF, and AW variants. The ratios of aspartate to maltose ring expansion rates generally were between 1.8 and 2.4 (Table 1), with the higher values associated with the receptors supporting the best aspartate taxis. However, the ratio for the WW receptor was 2.6, and the ratio for the WA receptor was 3.1, indicating that these receptors were selectively defective for maltose taxis.

Residue 210 Contributes Modestly to Tar_{Ec} Function When Residue 209 Is Trp. To examine the contribution of residue 210 to signal output when position 209 is occupied by the favored Trp residue, we constructed a series of Tar_{Ec} variants with different residue replacements at position 210 (Figure 4 and Table 2). All of the receptors supported aspartate taxis, with ring expansion rates ranging from 1.3 mm/h for the

Table 1. Relative Rates of Migration of VB13 Cells Expressing the Tar_{Ec} Variants in Semisolid (swim) Agar Containing Aspartate or Maltose

receptor	AA	AF	AW	AY	FA	FF	FW	FY
Asp[a]	79 ± 1.9	59 ± 1.1	60 ± 1.1	52 ± 1.0	91 ± 1.3	66 ± 2.2	87 ± 2.4	81 ± 3.1
Mal[a]	88 ± 2.1	79 ± 1.5	74 ± 1.4	68 ± 1.3	98 ± 1.4	78 ± 2.6	94 ± 2.6	102 ± 3.9
Asp:Mal ratio[b]	2.2 ± 0.05	1.8 ± 0.03	2.0 ± 0.04	1.8 ± 0.04	2.2 ± 0.03	2.0 ± 0.07	2.2 ± 0.06	1.9 ± 0.07
receptor	WA	WF	WW	**WY**	YA	YF	YW	YY
Asp[a]	108 ± 3.6	112 ± 3.3	103 ± 4.7	**100 ± 2.2**	80 ± 2.7	73 ± 1.9	88 ± 2.8	82 ± 3.2
Mal[a]	114 ± 2.8	114 ± 3.4	93 ± 4.3	**100 ± 2.2**	95 ± 3.3	84 ± 2.2	96 ± 3.1	92 ± 3.5
Asp:Mal ratio[b]	3.1 ± 0.10	2.4 ± 0.07	2.6 ± 0.12	**2.4 ± 0.05**	2.1 ± 0.07	2.1 ± 0.05	2.2 ± 0.07	2.2 ± 0.08

[a]The means and standard error of the rate of migration for VB13 cells expressing various receptors were normalized to that of VB13 cells expressing wild-type (WY) Tar_{Ec}. The wild type (WY) is underlined, and its values are shown in bold. Error values for aspartate and maltose represent the propagated error upon normalization of the data to VB13 cells harboring pBR322 and expressing the wild-type receptor. [b]The Asp:Mal ratio is the rate of expansion of the aspartate chemotaxis ring divided by the rate of expansion of the maltose chemotaxis ring. The error values for the Asp:Mal ratio represent the propagated error from the previous calculations.

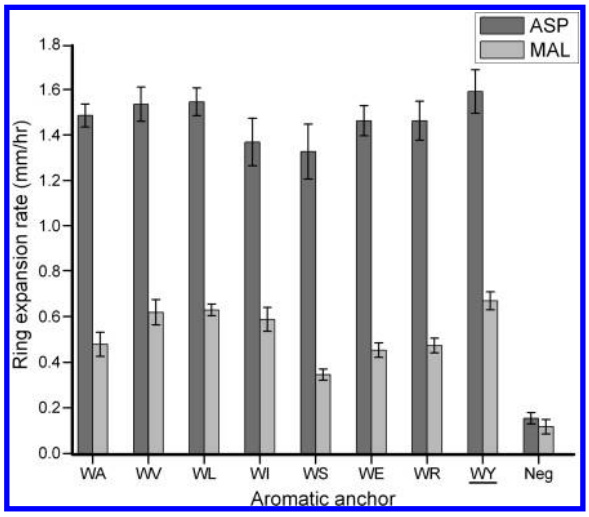

Figure 4. Chemotaxis ring formation in aspartate and maltose swim plates by cells expressing Tar_{Ec} with Trp-209 and various different residues at position 210. The measurements of ring expansion rates were performed as described in the legend of Figure 3. The error bars represent the standard deviation of the mean for the expansion rates of at least six colonies. The wild-type anchor (WY) is underlined.

WS variant to 1.5 mm/h for the WL and WV variants. However, larger differences were seen for maltose taxis. With the WL and WV receptors, the expansion rates were similar to the wild-type rate of 0.65 mm/h, and only slightly lower (0.6 mm/h) for the WI variant. However, with the WE and WR receptors, the expansion rates were only 0.45 mm/h, and only 0.36 mm/h for the WS variant. The ratios of the aspartate to maltose ring expansion rates ranged from 2.3 mm/h for cells expressing the WI receptor to 3.7 for cells expressing the WS receptor.

None of the WX receptors differed significantly from wild-type Tar_{Ec} in their baseline levels of covalent modification or in changes in the modification state seen after addition of aspartate or $NiSO_4$ (Figure S6 of the Supporting Information). We therefore anticipated that they would support essentially wild-type patterns of rotational bias and switching frequency. Analysis of tethered HCB436 cells expressing the different receptors confirmed this prediction (Figure S7 of the Supporting Information). We conclude that, when Trp is present at position 209, the residue at position 210 has relatively little effect on receptor function unless it is charged (Glu or Arg) or uncharged but highly polar (Ser).

DISCUSSION

E. coli chemoreceptors are membrane-spanning enzymes with multiple allosteric inputs,[47] including ligand binding, covalent modification, and interaction with other receptors and Che proteins. The relatively small energetic contributions of these inputs strongly suggest that the receptors exist in metastable states and are poised to respond to small changes. The binding of a ligand to the periplasmic domain must be communicated through the cell membrane to the signal-processing HAMP domain via TM2. It is therefore clear that the TM2 of a particular receptor must evolve to undergo conformational changes that are driven by the binding energy of their respective ligands.

The dynamic bundle model for function of the HAMP domain during chemoreceptor signaling[48,49] suggests that the stability of the HAMP domain is regulated by its attachment to TM2 via a five-residue linker, called the control cable.[18,49] Previously published experimental data[24−26] and a recent

Table 2. Relative Rates of Migration of VB13 Cells Expressing Tar_{Ec} WX Aromatic Anchor Variants in Semisolid (swim) Agar Containing Aspartate or Maltose

	WA	WV	WL	WI	WS	WE	WR	WY
Asp[a]	93 ± 5.6	96 ± 5.8	97 ± 5.8	86 ± 5.2	83 ± 5.1	92 ± 5.5	92 ± 5.5	**100 ± 5.9**
Mal[a]	72 ± 4.2	92 ± 5.4	94 ± 5.5	88 ± 5.1	53 ± 3.1	68 ± 4.0	71 ± 4.1	**100 ± 5.8**
Asp:Mal ratio[b]	3.1 ± 0.34	2.5 ± 0.22	2.4 ± 0.10	2.3 ± 0.2	3.7 ± 0.33	3.2 ± 0.23	3.1 ± 0.21	**2.4 ± 0.14**

[a]The means and standard deviations of the rate of migration for VB13 cells expressing various receptors were normalized to that of VB13 cells expressing wild-type (WY) Tar_{Ec}. The wild type (WY) is underlined, and its values are shown in bold. Error values for aspartate and maltose conditions represent the propagated error upon normalization of the data to VB13 cells harboring pBR322 and expressing the wild-type receptor. [b]The Asp:Mal ratio is the rate of expansion of the aspartate chemotaxis ring divided by the rate of expansion of the maltose chemotaxis ring. The error values for the Asp:Mal ratio represent the propagated error from the previous calculations.

dx.doi.org/10.1021/bi201555x | *Biochemistry* 2012, 51, 1925−1932

computer simulation[50] suggest that the aromatic anchor of TM2 is essential for normal transmembrane signaling. The work reported here indicates that one function of the aromatic anchor is to maintain a receptor in a baseline signaling state that allows both kinase-inhibiting (attractant) and kinase-stimulating (repellent) signals to be sensed with high sensitivity and a wide dynamic range. Although changes in the baseline signaling state can be compensated by increasing or decreasing the state of covalent modification, as appropriate, such adjustments displace the receptor from its properly poised baseline signaling state. The dynamic range of a receptor with an inappropriate aromatic anchor may be limited by the initially skewed state of covalent modification, and the mutant receptor may no longer be maximally responsive to the energy input provided by the binding of its particular ligand(s).

Our variant Tar_{Ec} receptors provide evidence of both types of disruption to receptor function. All receptors that lack Trp at position 209 have baseline signaling states shifted toward a kinase-inhibiting, attractant-mimicking configuration (Figure 1). With all of these receptors, some level of CW rotation could be restored by an increased level of covalent modification (Figures S2 and S3 of the Supporting Information), but these receptors are all defective, to varying degrees, in supporting aspartate and maltose taxis (Figure 3). Receptors with the highest baseline modification state were the most defective for chemotaxis.

A second, more subtle disruption is evidenced by receptors that have Trp at position 209 but lack an aromatic or aliphatic residue at position 210. The WA, WR, WE, and WS receptors all were able to mediate essentially normal aspartate taxis, and they showed wild-type patterns of covalent modification in the baseline state. However, these four receptors were all selectively defective for maltose taxis (Figure 4). We propose that this is because the energy supplied by interaction of the periplasmic domain of Tar_{Ec} with ligand-bound MBP is lower than the energy supplied by interaction with aspartate. This result is based on the stronger response of *E. coli* to aspartate than to maltose in capillary assays, the longer response times to addition of aspartate than to addition of maltose in tethered cell assays, and the ability of aspartate to completely block the response to maltose in certain competition assays.[51,52] In terms of a mechanical analogy, against whose overuse we have cautioned,[53] the spring constant resisting the pistonlike movement of helix 4 of TM2 is greater for the WA, WE, WR, and WS receptors.

Our current model for the function of the cytoplasmic aromatic anchor is illustrated in the diagram in Figure 5. In the wild-type receptor in the absence of ligand, a postulated inward-directed force on TM2 is balanced by a restoring force of the WY cytoplasmic anchor (Figure 5A), and the receptor is maintained in an alternating CW/CCW signaling state. The other WX anchors apparently exert a similar restoring force. When the attractant binds, the inward force imposed by the periplasmic domain increases, the balancing force of the cytoplasmic anchor is overcome, and TM2 is displaced inward (Figure 5B). The result is that the receptor is converted into a CCW signaling state. Binding of a repellent exerts an opposite, outward-directed force that results in CW signaling (Figure 5C). Moving the WY anchor one residue in the C-terminal direction (the +1 receptor[26]) generates a stronger outward-directed force that also leads to CW signaling (Figure 5D). Moving the WY anchor one residue in the N-terminal direction (the −1 receptor[26]) generates an inward-directed force that

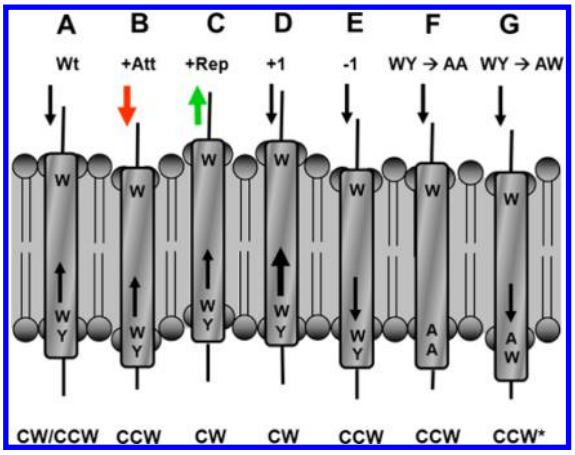

Figure 5. Model for the role of the cytoplasmic aromatic anchor of TM2 in transmembrane signaling. (A) In the wild-type (WT) receptor, a weak inward-directed force (thin downward arrow) exerted by the periplasmic domain is balanced by a weak outward-directed force (thin upward arrow) caused by the energetic cost of moving the WY tandem pair from the hydrophobic−polar interface at the cytoplasmic surface of the membrane. The receptor remains in a CW/CCW-balanced signaling state. (B) When an attractant binds to the periplasmic domain, the inward-directed force (red arrow) becomes greater, and TM2 is displaced inward, leading to CCW signaling. The membrane surfaces may also be slightly deformed. (C) When a repellent binds, an outward-directed force (green arrow) is exerted by the periplasmic domain, and TM2 is displaced outward, leading to CW signaling. Again, the membrane surfaces may be slightly deformed. (D) When the WY tandem pair is shifted one position toward the C-terminus (+1), the upward restoring force imposed by the aromatic anchor increases (bold black upward arrow), and a CW signaling state is favored. (E) When the WY tandem pair is shifted one position toward the N-terminus (−1), the inward force exerted by the periplasmic domain is augmented by an inward-directed force generated by the displaced aromatic anchor (lower thin downward arrow), leading to a CCW signaling state. (F) When the cytoplasmic aromatic anchor is weakened by replacement of the WY tandem pair with AA, there is no resistance to the inward force exerted by the periplasmic domain, and the receptor is shifted toward a CCW signaling state. (G) When the WY tandem pair of the cytoplasmic aromatic anchor is replaced the AW pair, there is an additional inward-directed force (lower thin downward arrow) induced by the C-terminally shifted Trp residue, and the inward-directed force is augmented to lead to a more strongly CCW signaling state, designated as CCW*.

leads to CCW signaling (Figure 5E). When the aromatic anchor is removed (the AA receptor), the restoring force is eliminated and the inward-directed force imposed by the periplasmic domain dominates, leading to CCW signaling (Figure 5F). Finally, when Trp-209 is replaced with Ala and an aromatic residue is retained at position 210 (e.g., the AW receptor), the displaced aromatic anchor may interact additively with the inward-directed force exerted by the periplasmic domain to create an even stronger CCW (CCW*) signaling bias (Figure 5G). In all cases of CCW signaling bias, an increased level of covalent modification can restore the CW/CCW signaling state in a $cheR^+B^+$ cell.

The known TM2 sequences of MCPs in *E. coli* and two other enteric bacteria, *Salmonella enterica* and *Enterobacter aerogenes*, are given in Table S1 of the Supporting Information. All of the MCPs that have a C-terminal pentapeptide CheR-binding motif ($NWE^S/_TF$) have Trp residues at the hydrophobic−polar interfaces of the both the periplasmic and the cytoplasmic

membrane surfaces. These receptors are the most important for determining the baseline signaling state of the receptor patch, and they are typically the most abundant of the chemoreceptors. It therefore seems reasonable that they are the ones for which the position of TM2 relative to the membrane would need to be most tightly regulated.

The remaining MCPs have a more variable TM2 composition, although they all have aromatic residues at the C-terminal end of the TM2 core region. The same is true of the TM2 core regions of the histidine protein kinases (HPKs) NarX, NarQ, PhoQ, and EnvZ, and of the Aer redox chemoreceptor, all of which also have a HAMP domain that follows closely after their TM2 helices. It may be that the precise positioning of TM2 is less critical for these proteins. For the lower-abundance MCPs and Aer, this could be because they exist in mixed patches with the high-abundance MCPs, which might dictate the signaling states of the mixed trimers of dimers.[54] For histidine kinases that regulate gene expression on a time scale of minutes or hours, fine control of their activity on a short time scale may not be as important a consideration as it is for chemoreceptors that mediate responses on a scale of a few seconds.

Functional hybrids can be made between the sensing and signal output domains of different chemoreceptors [Tsr-Tar and Tar-Tsr,[55] Trg-Tsr,[56] Tap-Tar,[36] and between an HPK-sensing domain and a chemoreceptor output domain (NarX-Tar[42,57])]. Because all of these proteins mediate effective chemotaxis when they are present as the sole MCP in a cell, adaptive covalent modification must be able to accommodate whatever defects there may be in their function. Perhaps some of them would not support normal CW/CCW rotation biases in Δ*cheRB* cells. It is reasonable to propose that the precise composition and placement of the cytoplasmic aromatic anchor of TM2 determine the baseline signaling state and the energy input required for transmembrane signaling. Thus, the aromatic anchor and the ligand-binding site should coevolve to provide optimal performance for each receptor type.

■ ASSOCIATED CONTENT

Supporting Information

Additional results and controls relating to swarm plates, the methylation state of receptors, and the bias of a cell containing wild-type and/or mutant receptors. This material is available free of charge via the Internet at http://pubs.acs.org.

■ AUTHOR INFORMATION

Corresponding Author

*Department of Biology, Texas A&M University, 3258 TAMUS, College Station, TX 77843-3258. Telephone: (979) 845-5158. Fax: (979) 845-2891. E-mail: mike@mail.bio.tamu.edu.

Funding

Early stages of this work were funded by the National Institutes of Health (GM39736). Recent funding has come from the Bartoszek Fund for Basic Biological Science. R.R.D. was supported by a Kirschstein National Research Service Award (AI075773) and by the German Research Foundation (SFB807, Transport and Communication across Biological Membranes).

Notes

The authors declare no competing financial interest.

■ ACKNOWLEDGMENTS

We thank the many undergraduates that worked with us during the initial stages of this project, notably Buddath Chy, Cameron Shokri, and Bilal Shamsi. The anti-flagellar antibody used for tethering cells was a gift from Sandy Parkinson. Lily Bartoszek proofread the final version of the manuscript before submission.

■ REFERENCES

(1) Welch, M., Oosawa, K., Aizawa, S., and Eisenbach, M. (1993) Phosphorylation-dependent binding of a signal molecule to the flagellar switch of bacteria. *Proc. Natl. Acad. Sci. U.S.A. 90*, 8787−8791.

(2) Silverman, M., and Simon, M. (1974) Flagellar rotation and the mechanism of bacterial motility. *Nature 249*, 73−74.

(3) Berg, H. C., and Brown, D. A. (1972) Chemotaxis in *Escherichia coli* analysed by three-dimensional tracking. *Nature 239*, 500−504.

(4) Macnab, R. M., and Koshland, D. E. Jr. (1972) The gradient-sensing mechanism in bacterial chemotaxis. *Proc. Natl. Acad. Sci. U.S.A. 69*, 2509−2512.

(5) Hazelbauer, G. L., Falke, J. J., and Parkinson, J. S. (2008) Bacterial chemoreceptors: High-performance signaling in networked arrays. *Trends Biochem. Sci. 33*, 9−19.

(6) Springer, W. R., and Koshland, D. E. (1977) Identification of a protein methyltransferase as the cheR gene product in the bacterial sensing system. *Proc. Natl. Acad. Sci. U.S.A. 74*, 533−537.

(7) Stock, J. B., and Koshland, D. E. (1978) A protein methylesterase involved in bacterial sensing. *Proc. Natl. Acad. Sci. U.S.A. 75*, 3659−3663.

(8) Kehry, M. R., Bond, M. W., Hunkapiller, M. W., and Dahlquist, F. W. (1983) Enzymatic deamidation of methyl-accepting chemotaxis proteins in *Escherichia coli* catalyzed by the cheB gene product. *Proc. Natl. Acad. Sci. U.S.A. 80*, 3599−3603.

(9) Bornhorst, J. A., and Falke, J. J. (2000) Attractant regulation of the aspartate receptor-kinase complex: Limited cooperative interactions between receptors and effects of the receptor modification state. *Biochemistry 39*, 9486−9493.

(10) Hazelbauer, G. L. (1975) The binding of maltose to 'virgin' maltose-binding protein is biphasic. *J. Bacteriol. 122*, 206−214.

(11) Spurlino, J. C., Lu, G. Y., and Quiocho, F. A. (1991) The 2.3 Å resolution structure of the maltose- or maltodextrin-binding protein, a primary receptor of bacterial active transport and chemotaxis. *J. Biol. Chem. 266*, 5202−5219.

(12) Gardina, P. J., Bormans, A. F., Hawkins, M. A., Meeker, J. W., and Manson, M. D. (1997) Maltose-binding protein interacts simultaneously and asymmetrically with both subunits of the Tar chemoreceptor. *Mol. Microbiol. 23*, 1181−1191.

(13) Gardina, P., Conway, C., Kossman, M., and Manson, M. (1992) Aspartate and maltose-binding protein interact with adjacent sites in the Tar chemotactic signal transducer of *Escherichia coli*. *J. Bacteriol. 174*, 1528−1536.

(14) Tso, W. W., and Adler, J. (1978) Negative chemotaxis in *Escherichia coli*. *J. Bacteriol. 118*, 560−576.

(15) Englert, D. L., Adase, C. A., Jayaraman, A., and Manson, M. D. (2010) Repellent taxis in response to nickel ion requires neither Ni^{2+} transport nor the periplasmic NikA binding protein. *J. Bacteriol. 192*, 2633−2637.

(16) Aravind, L., and Ponting, C. P. (1999) The cytoplasmic helical linker domain of receptor histidine kinase and methyl-accepting proteins is common to many prokaryotic signalling proteins. *FEMS Microbiol. Lett. 176*, 111−116.

(17) Hulko, M., Berndt, F., Gruber, M., Linder, J. U., Truffault, V., Schultz, A., Martin, J., Schultz, J. E., Lupas, A. N., and Coles, M. (2006) The HAMP domain structure implies helix rotation in transmembrane signaling. *Cell 126*, 929−940.

(18) Kitanovic, S., Ames, P., and Parkinson, J. S. (2011) Mutational Analysis of the Control Cable That Mediates Transmembrane Signaling in the *Escherichia coli* Serine Chemoreceptor. *J. Bacteriol. 193*, 5062−5072.

(19) Milburn, M. V., Privé, G. G., Milligan, D. L., Scott, W. G., Yeh, J., Jancarik, J., Koshland, D. E. Jr., and Kim, S. H. (1991) Three-dimensional structures of the ligand-binding domain of the bacterial aspartate receptor with and without a ligand. *Science 254*, 1342−1347.
(20) Chervitz, S. A., and Falke, J. J. (1995) Lock on/off disulfides identify the transmembrane signaling helix of the aspartate receptor. *J. Biol. Chem. 270*, 24043−24053.
(21) Hughson, A. G., and Hazelbauer, G. L. (1996) Detecting the conformational change of transmembrane signaling in a bacterial chemoreceptor by measuring effects on disulfide cross-linking *in vivo*. *Proc. Natl. Acad. Sci. U.S.A. 93*, 11546−11551.
(22) Ottemann, K. M., Xiao, W., Shin, Y. K., and Koshland, D. E. Jr. (1999) A piston model for transmembrane signaling of the aspartate receptor. *Science 285*, 1751−1754.
(23) Isaac, B., Gallagher, G. J., Balazs, Y. S., and Thompson, L. K. (2002) Site-directed rotational resonance solid-state NMR distance measurements probe structure and mechanism in the transmembrane domain of the serine bacterial chemoreceptor. *Biochemistry 41*, 3025−3036.
(24) Miller, A. S., and Falke, J. J. (2004) Side chains at the membrane-water interface modulate the signaling state of a transmembrane receptor. *Biochemistry 43*, 1763−1770.
(25) Draheim, R. R., Bormans, A. F., Lai, R.-Z., and Manson, M. D. (2005) Tryptophan residues flanking the second transmembrane helix (TM2) set the signaling state of the Tar chemoreceptor. *Biochemistry 44*, 1268−1277.
(26) Draheim, R. R., Bormans, A. F., Lai., R.-Z., and Manson, M. D. (2006) Tuning a Bacterial Chemoreceptor with Protein-Membrane Interactions. *Biochemistry 45*, 14655−14664.
(27) Yau, W. M., Wimley, W. C., Gawrisch, K., and White, S. H. (1998) The preference of tryptophan for membrane interfaces. *Biochemistry 37*, 14713−14718.
(28) Braun, P., and von Heijne, G. (1999) The aromatic residues Trp and Phe have different effects on the positioning of a transmembrane helix in the microsomal membrane. *Biochemistry 38*, 9778−9782.
(29) de Planque, M. R., and Killian, J. A. (2003) Protein-lipid interactions studied with designed transmembrane peptides: Role of hydrophobic matching and interfacial anchoring. *Mol. Membr. Biol. 20*, 271−284.
(30) Sevvana, M., Vijayan, V., Zweckstetter, M., Reinelt, S., Madden, D. R., Herbst-Irmer, R., Sheldrick, G. M., Bott, M., Griesinger, C., and Becker, S. (2008) A ligand-induced switch in the periplasmic domain of sensor histidine kinase CitA. *J. Mol. Biol. 377*, 512−523.
(31) Cheung, J., Le-Khac, M., and Hendrickson, W. A. (2009) Crystal structure of a histidine kinase sensor domain with similarity to periplasmic binding proteins. *Proteins 77*, 235−241.
(32) Moore, J. O., and Hendrickson, W. A. (2009) Structural analysis of sensor domains from the TMAO-responsive histidine kinase receptor TorS. *Structure 17*, 1195−1204.
(33) Zhang, Z., and Hendrickson, W. A. (2010) Structural characterization of the predominant family of histidine kinase sensor domains. *J. Mol. Biol. 400*, 335−353.
(34) Wolfe, A. J., and Berg, H. C. (1989) Migration of bacteria in semisolid agar. *Proc. Natl. Acad. Sci. U.S.A. 86*, 6973−6977.
(35) Smith, R. A., and Parkinson, J. S. (1980) Overlapping genes at the cheA locus of *Escherichia coli*. *Proc. Natl. Acad. Sci. U.S.A. 77*, 5370−5374.
(36) Weerasuriya, S., Schneider, B. M., and Manson, M. D. (1998) Chimeric chemoreceptors in *Escherichia coli*: Signaling properties of Tar-Tap and Tap-Tar hybrids. *J. Bacteriol. 180*, 914−920.
(37) Parkinson, J. S. (1978) Complementation analysis and deletion mapping of *Escherichia coli* mutants defective in chemotaxis. *J. Bacteriol. 135*, 45−53.
(38) Cantwell, B. J., Draheim, R. R., Weart, R. B., Nguyen, C., Stewart, R. C., and Manson, M. D. (2003) CheZ phosphatase localizes to chemoreceptor patches via CheA-short. *J. Bacteriol. 185*, 2354−2361.
(39) Southern, J. A., Young, D. F., Heaney, F., Baumgärtner, W. K., and Randall, R. E. (1991) Identification of an epitope on the P and V proteins of simian virus 5 that distinguishes between two isolates with different biological characteristics. *J. Gen. Virol. 72*, 1551−1557.
(40) Guzman, L. M., Belin, D., Carson, M. J., and Beckwith, J. (1995) Tight regulation, modulation, and high-level expression by vectors containing the arabinose PBAD promoter. *J. Bacteriol. 177*, 4121−4130.
(41) Miller, J. H. (1972) *Experiments in Molecular Genetics*, Cold Spring Harbor Laboratory Press, Plainview, NY.
(42) Ward, S. M., Bormans, A. F., and Manson, M. D. (2006) Mutationally altered signal output in the Nart (NarX-Tar) hybrid chemoreceptor. *J. Bacteriol. 188*, 3944−3951.
(43) Berg, H. C., and Block, S. M. (1984) A miniature flow cell designed for rapid exchange of media under high-power microscope objectives. *J. Gen. Microbiol. 130*, 2915−2920.
(44) Lai, R. Z., Manson, J. M., Bormans, A. F., Draheim, R. R., Nguyen, N. T., and Manson, M. D. (2005) Cooperative signaling among bacterial chemoreceptors. *Biochemistry 44*, 14298−14307.
(45) Bormans, A. (2005) Intradimer and Interdimer Methylation Response by Bacterial Chemoreceptors to Attractant Stimulus. Ph.D. Dissertation, Texas A&M University, College Station, TX.
(46) Goy, M. F., Springer, M. S., and Adler, J. (1978) Failure of sensory adaptation in bacterial mutants that are defective in a protein methylation reaction. *Cell 15*, 1231−1240.
(47) Manson, M. D. (2010) Bacterial chemoreceptors as membrane-spanning allosteric enzymes, In *Sensory Mechanisms in Bacteria: Molecular Aspects of Signal Recognition*. Spiro, S. and Dixon, R., Eds. Caister Academic Press, Norfolk, United Kingdom, pp 107−149.
(48) Zhou, Q., Ames, P., and Parkinson, J. S. (2009) Mutational analyses of HAMP helices suggest a dynamic bundle model of input-output signalling in chemoreceptors. *Mol. Microbiol. 73*, 801−814.
(49) Zhou, Q., Ames, P., and Parkinson, J. S. (2011) Biphasic control logic of HAMP domain signalling in the *Escherichia coli* serine chemoreceptor. *Mol. Microbiol. 80*, 596−611.
(50) Park, H., Im, W., and Seok, C. (2011) Transmembrane signaling of chemotaxis receptor tar: Insights from molecular dynamics simulation studies. *Biophys. J. 100*, 2955−2963.
(51) Gardina, P. J., Bormans, A. F., and Manson, M. D. (1998) A mechanism for simultaneous sensing of aspartate and maltose by the Tar chemoreceptor of *Escherichia coli*. *Mol. Microbiol. 29*, 1147−1154.
(52) Manson, M. D., and Kossmann, M. (1986) Mutations in tar suppress defects in maltose chemotaxis caused by specific malE mutations. *J. Bacteriol. 165*, 34−40.
(53) Manson, M. D. (2011) Transmembrane signaling is anything but rigid. *J. Bacteriol. 193*, 5059−5061.
(54) Ames, P., Studdert, C. A., Reiser, R. H., and Parkinson, J. S. (2002) Collaborative signaling by mixed chemoreceptor teams in *Escherichia coli*. *Proc. Natl. Acad. Sci. U.S.A. 99*, 7060−7065.
(55) Krikos, A., Conley, M. P., Boyd, A., Berg, H. C., and Simon, M. I. (1985) Chimeric sensory transducers of *Escherichia coli*. *Proc. Natl. Acad. Sci. U.S.A. 82*, 1326−1330.
(56) Feng, X., Baumgartner, J. W., and Hazelbauer, G. L. (1997) High- and Low-Abundance Chemoreceptors in *Escherichia coli*: Differential Activities Associated with Closely Related Cytoplasmic Domains. *J. Bacteriol. 170*, 6714−6720.
(57) Ward, S. M., Delgado, A., Gunsalus, R. P., and Manson, M. D. (2002) Chimeric chemoreceptors in *Escherichia coli*: Signaling properties of Tar-Tap and Tap-Tar hybrids. *J. Bacteriol. 180*, 914−920.